

STATIC AND DYNAMIC ANALYSES OF STIFFENED FOLDED LAMINATE COMPOSITE PLATE

Tran Ich Think¹, Bui Van Binh², Tran Minh Tu³

¹ Hanoi University of Science and Technology, Vietnam

² University of Power Electric, Vietnam

³ University of Civil Engineering, Vietnam

Abstract. This paper presents some numerical results of bending and vibration analyses of an unstiffened and stiffened folded laminate composite plate using finite element method. The effects of fiber orientations, boundary conditions, stiffener conditions of the plates for deflections, natural frequencies, and the corresponding mode shapes, transient displacement responses were considered. The Matlab programming using rectangular isoparametric plate element with five degree of freedom per node based on Mindlin plate theory was built to solve the problems. A good agreement is found between the results of this technique and other published results available in the literature.

Keywords: Bending, folded laminated composite plate, vibration, dynamic response, stiffeners, stiffened folded laminated composite plate, finite element.

1. INTRODUCTION

Many stiffened flat plates are designed to resist vibration due to dynamical loads. The effect of the stiffeners on the vibration behaviors of flat plates is known to be significant. Thus it is not surprising that a number of papers has been devoted to the study of this problem. Because the laminated plates with stiffeners become more and more important in the aerospace industry and other modern engineering fields, wide attention has been paid on the experimental, theoretical and numerical analysis for the static and dynamic problems of such structures in recent years. Turkmen and Mecitoglu [1] presented a numerical analysis and experimental study of stiffened laminated flat plates exposed to blast shock waves. Zhao et al. [2] using an energy approach, investigated the free vibration of the stiffened simply supported rotating cross-ply laminated cylindrical shells. Sadek and Tawfik [3] presented a higher-order finite element model and studied the behavior of concentrically and eccentrically stiffened laminated plates. Kumar and Mukhopadhyay [4] used mixing plane stress triangular element and discrete Kirchhoff-Mindlin plate bending element to investigate the stiffened laminated composite flat plates.

Olson and Hazell [5] have presented results from a theoretical and experimental comparison study on the vibration characteristics of all clamped and eccentrically stiffened isotropic flat plates. They used a triangular finite element in the calculations. Kalfi [6] developed a 9-noded rectangular plate element and 3-noded beam element; the beams are

placed along the plate nodal lines to analysis of stiffened laminated plates under transverse loading. Biswal and Ghosh [7] used 4-noded rectangular elements with seven degrees of freedom at each node for analysis of stiffened plates. Gangadhara Prusty [8] studied linear static analysis of composite hat-stiffened laminated shells using 8-noded rectangular plate element and 3-noded beam element.

All of those analyses only investigated for flat plate with stiffeners. The folded plate is not readily available. The folded plate with stiffeners can be used to open the range of engineering applications of laminated composite plate. Because, they are lightweight, easy to form and economical, and have a much higher load carrying capacity than flat plates.

Behavior of unstiffened isotropic folded plates has been studied previously by a host of investigators using a variety of approaches. Goldberg and Leve [9] developed a method based on elasticity. According to this method, there are four components of displacements at each point along the joints: two components of translation and a rotation, all lying in the plane normal to the joint, and a translation in the direction of the joint. The stiffness matrix is derived from equilibrium equations at the joints, while expanding the displacements and loadings into the Fourier series considering boundary conditions. Bar-Yoseph and Herscovitz [10] formulated an approximate solution for folded plates based on Vlassov's theory of thin-walled beams. According to this work, the structure is divided into longitudinal beams connected to a monolithic structure. Cheung [11] was the first author developed the finite strip method for analyzing isotropic folded plates. Additional works in the finite strip method have been presented. The difficulties encountered with the intermediate supports in the finite strip method [12] were overcome and subsequently Maleki [13] proposed a new method, known as compound strip method. Irie et al. [14] used Ritz method for the analysis of free vibration of an isotropic cantilever folded plate.

Perry et al. [15] presented a rectangular hybrid stress element for analyzing a isotropic folded plate structures in bending cases. In this, they used a four-node element, which is based on the classical hybrid stress method, is called the hybrid coupling element and is generated by a combination of a hybrid plane stress element and a hybrid plate bending element. Darilmaz et al. [16] presented an 8-node quadrilateral assumed-stress hybrid shell element. Their formulation is based on Hellinger-Reissner variational principle for bending and free vibration analyses of structures which have isotropic material properties.

For unstiffened composite folded plate, Haldar and Sheikh [17] presented a free vibration analysis of isotropic and composite folded plate by using a sixteen nodes triangular element. Suresh and Malhotra [18] studied the free vibration of damped composite box beams using four node plate elements with five degrees of freedom per node.

Recently, Niyogi et al. in [19] reported the analysis of unstiffened and stiffened symmetric cross-ply laminate composite folded plates using first-order transverse shear deformation theory and nine nodes elements. In their works, only in axis symmetric cross-ply laminated plates were considered. So that, there is uncoupling between the normal and shear forces, and also between the bending and twisting moments, then besides the above uncoupling, there is no coupling between the forces and moment terms. Tran Ich Thinh et al. in [20-23] presented a finite element method to analyze of bending, free vibration and time displacement response of V-shape; W-shape sections and multi-folding laminate

plate (which having trapezoidal corrugate plate). In these studies, the effects of folding angles, fiber orientations, loading conditions, boundary condition have been investigated.

In this paper, eight-noded isoparametric rectangular plate elements were used to analyze the stiffened folded laminate composite plate with in-axis configuration and off-axis configuration. Some numerical results for bending, natural frequencies, and dynamic responses of the plates under various fiber orientations, stiffener orientations, and boundary conditions are investigated.

2. THEORETICAL FORMULATION

2.1. Displacement and strain yield

According to the Reissner-Mindlin plate theory, the displacements (u, v, w) are referred to those of the mid-plane (u_0, v_0, w_0) as

$$\begin{Bmatrix} u \\ v \\ w \end{Bmatrix} = \begin{Bmatrix} u_0 + z\theta_x \\ v_0 + z\theta_y \\ w_0 \end{Bmatrix} \text{ and } \begin{Bmatrix} \theta_x \\ \theta_y \end{Bmatrix} = \begin{Bmatrix} \frac{\partial w}{\partial x} + \phi_x \\ \frac{\partial w}{\partial y} + \phi_y \end{Bmatrix} \quad (1)$$

Here, θ_x and θ_y are the total rotations, ϕ_x and ϕ_y are the constant average shear deformations about the y and x -axes, respectively. The z -axis is normal to the xy -plane that coincides with the mid-plane of the laminate positive downward and clockwise with x and y . The generalized displacement vector at the mid-plane can thus be defined as

$$\{d\} = \{u_0, v_0, w_0, \theta_x, \theta_y\}^T$$

The strain-displacement relations can be taken as

$$\begin{Bmatrix} \epsilon_{xx} \\ \epsilon_{yy} \\ \epsilon_{zz} \\ \gamma_{xy} \\ \gamma_{yz} \\ \gamma_{xz} \end{Bmatrix} = \begin{Bmatrix} \frac{\partial u_0}{\partial x} + z \frac{\partial \theta_x}{\partial x} \\ \frac{\partial v_0}{\partial y} + z \frac{\partial \theta_y}{\partial y} \\ 0 \\ \left(\frac{\partial u_0}{\partial y} + \frac{\partial v_0}{\partial x} \right) + z \left(\frac{\partial \theta_x}{\partial y} + \frac{\partial \theta_y}{\partial x} \right) \\ \frac{\partial w_0}{\partial y} + \theta_y \\ \frac{\partial w_0}{\partial x} + \theta_x \end{Bmatrix} \quad (2)$$

2.2. Finite element formulations

The Hamilton variational principle is used here to derive the laminate equations of motion. The mathematical statement of the Hamilton principle in the absence of damping can be written as [24]

$$\int_{t_1}^{t_2} \delta \left(\frac{1}{2} \int_V \rho \{\dot{u}\}^T \{\dot{u}\} dV - \frac{1}{2} \int_V \{\varepsilon\}^T \{\sigma\} dV - \left(\int_V \{u\}^T \{f_b\} dV + \int_S \{u\}^T \{f_s\} dS + \{u\}^T \{f_c\} \right) \right) dt = 0 \quad (3)$$

In which

$$T = \frac{1}{2} \int_V \rho \{\dot{u}\}^T \{\dot{u}\} dV; \quad U = \frac{1}{2} \int_V \{\varepsilon\}^T \{\sigma\} dV;$$

$$W = \int_V \{u\}^T \{f_b\} dV + \int_S \{u\}^T \{f_s\} dS + \{u\}^T \{f_c\}$$

U, T are the potential energy, kinetic energy; W is the work done by externally applied forces. $u = [u, v, w]^T$ is the displacement of any generic point (x, y, z) in space.

In laminated plate theories, the membrane $\{N\}$, bending moment $\{M\}$ and shear stress $\{Q\}$ resultants can be obtained by integration of stresses over the laminate thickness. The stress resultants-strain relations can be expressed in the form

$$\begin{Bmatrix} \{N\} \\ \{M\} \\ \{Q\} \end{Bmatrix} = \begin{bmatrix} [A_{ij}] & [B_{ij}] & [0] \\ [B_{ij}] & [D_{ij}] & [0] \\ [0] & [0] & [F_{ij}] \end{bmatrix} \begin{Bmatrix} \{\varepsilon^0\} \\ \{\kappa\} \\ \{\gamma^0\} \end{Bmatrix} \quad (4)$$

where

$$([A_{ij}] \cdot [B_{ij}] \cdot [D_{ij}]) = \sum_{k=1}^n \int_{h_{k-1}}^{h_k} ([Q'_{ij}]_k) (1, z, z^2) dz, \quad i, j = 1, 2, 6 \quad (5)$$

$$[F_{ij}] = \sum_{k=1}^n f \int_{h_{k-1}}^{h_k} ([C'_{ij}]_k) dz; \quad f = 5/6; \quad i, j = 4, 5 \quad (6)$$

n : number of layers, h_{k-1}, h_k : the position of the top and bottom faces of the k^{th} layer. $[Q'_{ij}]_k$ and $[C'_{ij}]_k$: reduced stiffness matrices of the k^{th} layer (see [25, 26]).

In the present work, the eight noded isoparametric quadrilateral element with five degrees of freedom per nodes is used. The displacement field of any point on the mid-plane is given by

$$u_0 = \sum_{i=1}^8 N_i(\xi, \eta) u_i; \quad v_0 = \sum_{i=1}^8 N_i(\xi, \eta) v_i; \quad w_0 = \sum_{i=1}^8 N_i(\xi, \eta) w_i;$$

$$\theta_x = \sum_{i=1}^8 N_i(\xi, \eta) \theta_{xi}; \quad \theta_y = \sum_{i=1}^8 N_i(\xi, \eta) \theta_{yi} \quad (7)$$

where $N_i(\xi, \eta)$ are the shape function associated with node i in terms of natural coordinates (ξ, η) . The strain field so that can be expressed as

$$\{\epsilon^o\} = \begin{Bmatrix} \epsilon_{xx}^o \\ \epsilon_{yy}^o \\ \epsilon_{xy}^o \\ \kappa_x \\ \kappa_y \\ \kappa_{xy} \\ \gamma_{yz}^o \\ \gamma_{xz}^o \end{Bmatrix} = \begin{bmatrix} \frac{\partial}{\partial x} & 0 & 0 & 0 & 0 \\ 0 & \frac{\partial}{\partial y} & 0 & 0 & 0 \\ \frac{\partial}{\partial y} & \frac{\partial}{\partial x} & 0 & 0 & 0 \\ 0 & 0 & 0 & z \frac{\partial}{\partial x} & 0 \\ 0 & 0 & 0 & 0 & z \frac{\partial}{\partial y} \\ 0 & 0 & 0 & z \frac{\partial}{\partial y} & z \frac{\partial}{\partial x} \\ 0 & 0 & \frac{\partial}{\partial y} & 0 & 1 \\ 0 & 0 & \frac{\partial}{\partial x} & 1 & 0 \end{bmatrix} \begin{Bmatrix} u^o \\ v^o \\ w^o \\ \theta_x \\ \theta_y \end{Bmatrix} = [\partial] \begin{Bmatrix} u^o \\ v^o \\ w^o \\ \theta_x \\ \theta_y \end{Bmatrix}$$

$$= [\partial] [N_i] \{q_e\} = [B]_{8 \times 40} \{q_e\}$$

The element stiffness matrix is given by equation

$$[k]_{e(40 \times 40)} = \int_{A_e} ([B]^T)_{40 \times 8} |H|_{8 \times 8} |B|_{8 \times 40} t dA_e \quad (8)$$

In which $[B] = \{[B_1] [B_2] [B_3] [B_4] [B_5] [B_6] [B_7] [B_8]\}$

$$[B_i] = \begin{bmatrix} \frac{\partial N_i}{\partial x} & 0 & 0 & 0 & 0 \\ 0 & \frac{\partial N_i}{\partial y} & 0 & 0 & 0 \\ \frac{\partial N_i}{\partial y} & \frac{\partial N_i}{\partial x} & 0 & 0 & 0 \\ 0 & 0 & 0 & \frac{\partial N_i}{\partial x} & 0 \\ 0 & 0 & 0 & 0 & \frac{\partial N_i}{\partial y} \\ 0 & 0 & 0 & \frac{\partial N_i}{\partial y} & \frac{\partial N_i}{\partial x} \\ 0 & 0 & \frac{\partial N_i}{\partial y} & 0 & N_i \\ 0 & 0 & \frac{\partial N_i}{\partial x} & N_i & 0 \end{bmatrix}$$

The element stiffness matrix is given by

$$[k]_e = \int_{A_e} ([B]^T) [H] [B] t dA_e \quad (9)$$

where $[H]$ is the material stiffness matrix given by $[H] = \begin{bmatrix} [A_{1j}] & [B_{1j}] & 0 \\ [B_{1j}] & [D_{1j}] & 0 \\ 0 & 0 & [F_{1j}] \end{bmatrix}$

The element mass matrix is given by

$$[m]_e = \int_{A_e} \rho [N_i]^T [\bar{m}] [N_i] dA_e \quad (10)$$

With ρ is mass density of material.

$$[\bar{m}] = \begin{bmatrix} I_0 & 0 & 0 & I_1 & 0 \\ 0 & I_0 & 0 & 0 & I_1 \\ 0 & 0 & I_0 & 0 & 0 \\ I_1 & 0 & 0 & I_2 & 0 \\ 0 & I_1 & 0 & 0 & I_2 \end{bmatrix} \text{ and } I_i = \sum_1^8 \sum_{h_k}^{h_{k+1}} z' \rho dz, \quad i = 0, 1, 2. \quad (11)$$

Nodal force vector is expressed as

$$\{f\}_e = \int_{A_e} [N_i]^T q dA_e \quad (12)$$

Where q is the intensity of the applied load. For free and forced vibration analysis, the damping effect is neglected then the governing equations are [23]:

$$[\lambda] \{ \ddot{u} \} + [K] \{ u \} = \{ 0 \} \text{ or } \{ [\lambda] - \omega^2 [K] \} = \{ 0 \} \quad (13)$$

And

$$[\lambda] \{ \ddot{u} \} + [K] \{ u \} = f(t) \quad (14)$$

In which $\{ u \}$, $\{ \ddot{u} \}$ are the global vectors of unknown nodal displacement, acceleration, respectively. $[\lambda]$, $[K]$, $f(t)$ are the global mass matrix, stiffness matrix, applied load vectors, respectively.

$$[\lambda] = \sum_1^n [m^*]_e; \quad [K] = \sum_1^n [k^*]_e; \quad \{ f(t) \} = \sum_1^n \{ f_e^*(t) \} \quad (15)$$

In which $[m^*]_e = [T]^T [m]_e [T]$; $[k^*]_e = [T]^T [k]_e [T]$; $\{ f_e^*(t) \} = [T]^T \{ f \}_e$.

With n is the number of element.

In this analysis, both of stiffener and folded plates are modeled by eight-noded isoparametric rectangular plate element, the membrane and bending terms are coupled, as can be clearly seen in Fig. 1. Even more since a rotation of the normal appear as unknowns for the Reissner-Mindlin model, it is necessary to introduce a new unknown for the in-plane rotation called drilling degree of freedom, θ_z . The rotation θ_z at a node is not measured and does not contribute to the strain energy stored in the element [23, 27]. The technique is used here: Before applying the transformation, the 40×40 stiffness and mass

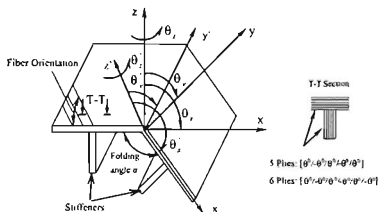


Fig. 1. Global x, y, z and local x', y', z' axes system for folded plate element, folding angle α

matrices are expanded to 48×48 sizes, to insert sixth θ_z drilling degrees of freedom at each node of a finite element. The off-diagonal terms corresponding to the θ_z terms are zeroes, while a very small positive number, we taken the θ_z equal to 10^{-4} times smaller than the smallest leading diagonal, is introduced at the corresponding leading diagonal term. The load vector is similarly expanded by using zero elements at corresponding locations. So that, for a folded element, the displacement vector of each node is [20, 23]:

$$\{u\} = [T] \{u'\} \quad (16)$$

where $u' = [u', v', w']^T$ is the displacement of a generic point in local coordinate system (x', y', z') .

$$[T] = \begin{bmatrix} l_{x'x} & l_{y'x} & l_{z'x} & 0 & 0 & 0 \\ l_{x'y} & l_{y'y} & l_{z'y} & 0 & 0 & 0 \\ l_{x'z} & l_{y'z} & l_{z'z} & 0 & 0 & 0 \\ 0 & 0 & 0 & l_{y'y} & -l_{x'y} & l_{z'y} \\ 0 & 0 & 0 & -l_{y'x} & l_{x'x} & -l_{z'x} \\ 0 & 0 & 0 & l_{y'z} & -l_{x'z} & l_{z'z} \end{bmatrix}$$

is the transformation matrix.

l_{ij} are the direction cosines between the global and local coordinates.

3. NUMERICAL RESULTS

Based on the foregoing theoretical formulation, a homemade Matlab code has been developed to calculate deflections, natural frequencies and investigating the mode shapes, transient displacement response of the folded composite plates with and without stiffeners. The stiffeners are modeled as laminated plate elements. In transient analysis, the Newmark method is used with parameters that control the accuracy and stability of $\alpha = 0.25$ and $\delta = 0.5$ (see [23]).

3.1. Validation examples

3.1.1. Example 1: Isotropic stiffened flat plate

Firstly, to observe the accuracy of the present Matlab code, the isotropic stiffened flat plate plotted in Fig. 2 is recalculated, which is a previously reported experimental and theoretical example (Olson and Hazell, 1977; Pal and Niyogi, 2008). Dimension parameters of the plate are illustrated with $L = W = 203$ mm, thickness of stiffener is 6.35 mm; width of stiffener is 12.7 mm; elastic modulus $E = 68.7$ GPa, Poisson ratio $\nu = 0.3$, density $\rho = 2820$ kg/m³. The results are compared with numerical results given by Olson [5], Pal et al. [19], and experimentally results given by Hazell [5]. In [5], the stiffener is modeled by beam elements, in [19] the stiffener is modeled by nine nodes elements.

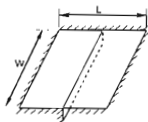


Fig. 2. Stiffened flat plate

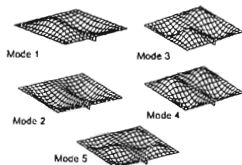


Fig. 3. First five mode shapes of stiffened flat plate

The first five natural frequencies obtained from the present code and those obtained by Olson, Pal et al. Hazell are present in Tab. 1. The first five mode shapes are shown in Fig.3. The results show a good agreement.

Table 1 Five first natural frequencies of isotropic stiffened flat plate

Mode	Frequency (Hz)	Numerical results		Experiment results
	Present	[19]	[5]	[5]
1	721.83	720.0	718.1	689
2	749.88	746.5	751.4	725
3	989.71	988.5	997.4	961
4	999.21	998.3	1007.1	986
5	1407.56	1405.9	1419.8	1376

In [5] (Olson and Hazell, 1977), the plate portion of the stiffened panels was modeled by triangular elements and the stiffeners were modeled by refined beam bending and torsion elements. Both in-plane and bending motions in the plate were considered, but in-plane inertias were neglected. The reasons need to be further investigated. The transverse

shear deformation, the rotary inertia of plate and stiffeners are considered in the present method. It is obvious that the current model is more advanced.

3.1.2. Example 2: Isotropic folded plate

In this example, the five folds folded plate structure illustrated in Fig. 4 is recalculated, which is a previously reported by Perry et al. [15] (1992) using a rectangular hybrid shell element and by Darilmaz et al. [16] (2006), using an 8-node assumed stress hybrid element. The dimensions of the structure are of $L = 1$ m; the width of $L_2 = L$; and thickness of $t = 0.05$ m.

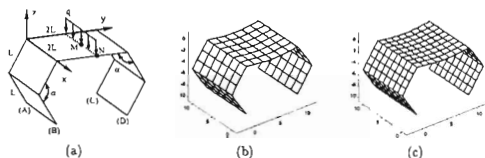


Fig. 4. Five first mode shapes of stiffened flat plate, (a) Geometry of the plate with two edges AB and CD simply supported, (b) Deformed plate with 108 elements, (c) Deformed plate with 192 elements

Table 2. Comparison of deflection (w) at points M and N and convergence of natural frequencies (Hz) for the five folds folded plate with simply supported edges

Number of elements	Source	Deflections		Natural frequencies (Hz)			
		w_M	w_N	f_1	f_2	f_3	f_4
48	Perry et al.[15]	-0.12171	-0.13101	-	-	-	-
	ANSYS [15]	-0.12180	-0.12940	-	-	-	-
	Darilmaz et al [16]	-0.12133	-0.12842	-	-	-	-
	Present	-0.12378	-0.13446	2.82	12.86	14.54	27.63
108	Present	-0.12229	-0.13389	2.78	12.76	14.38	27.47
192	Perry et al.[15]	-0.12177	-0.13114	-	-	-	-
	ANSYS [15]	-0.12170	-0.13050	-	-	-	-
	Darilmaz et al [16]	-0.12163	-0.13043	-	-	-	-
	Present	-0.12243	-0.13353	2.78	12.76	14.39	27.46

The boundary condition: two edges AB and CD: simply supported: $u = v = w = \theta_x = 0$. Knife-edge loading ($q = 100$ kN/m) of the center line of the upper plate is considered for static analysis. The material properties used are as: $E = 2.1 \times 10^6$ N/cm², $\nu = 0.3$.

Because the compatible finite elements are used, the natural frequencies should converge to the values of the mathematical model, as the number of elements is increased.

The results, as listed in Tab. 2, show that the reasonable convergence has been achieved with relatively small decrements in the first four frequencies,ts.

In the subsequent finite element models, the plate is divided by 192 eight-noded isoparametric rectangular plate elements. In Tab. 2. deflections at point M and N obtained by Perry et al. [15] and Darilmaz et al. [16] are given together with the present results for comparison. It is observed that the deflections are in good agreement.

In the following subsections, several new numerical examples have been analyzed.

3.2. Study cases of: folded laminated plate

Consider a five folds folded composite plate shown in Fig. 5, the material properties are shown in Tab. 3, $L = 1$ m, total thickness $t = 0.02$ m, folding angle $\alpha = 120^\circ$. Lamination schemes: symmetric and anti-symmetric in-axis configurations $[0^\circ/90^\circ/0^\circ/90^\circ/0^\circ]$; $[0^\circ/90^\circ/0^\circ/90^\circ/0^\circ/90^\circ]$ and off-axis configurations $[\theta^\circ/-\theta^\circ/\theta^\circ/-\theta^\circ/\theta^\circ]$; $[\theta^\circ/-\theta^\circ/\theta^\circ/-\theta^\circ/\theta^\circ/-\theta^\circ]$ are constructed. The reasons that we are take the configurations to investigate in this section are [26]: For symmetric laminates, from the definition of $[B_{ij}]$ (see Eq. (5)) matrix, it can be proved $|B_{ij}| = 0$. So that, there is uncoupling between the bending deformations and shear strains. Add-on. if the plate has an in-axis configurations, it is not only symmetric, giving $|B_{ij}| = 0$, but also $A_{16} = A_{26} = B_{16} = B_{26} = D_{16} = D_{26} = 0$. So that, there is also uncoupling between the bending and twisting. For anti-symmetric laminate, the matrix $[B_{ij}]$ is not equal to zero and if it consists of alternating $+\theta$ and $-\theta$ plies, the plate has higher shear stiffness and shear strength properties.

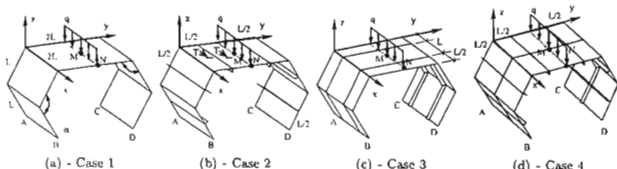


Fig. 5. Geometry of stiffened folded composite plate and knife-edge loading conditions

Table 3. Graphite-Epoxy (AS4/3501) material properties.

E_1 (GPa)	E_2 (GPa)	G_{12} (GPa)	G_{23} (GPa)	G_{13} (GPa)	ν_{12}	ρ (kg/m ³)
144.8	9.67	4.14	3.45	4.14	0.3	1500

Four following cases for different stiffener orientations are studied:

Case 1. Unstiffened folded composite plate (Fig. 5a), including 192 elements.

Case 2. Six x -stiffeners are attached below the folded plate running along the length of the clamped edges (Fig. 5b) with total mass increment of 10% (width of stiffening plate taken equal to 5cm and thickness remaining same as the original folded plate) with 192 of elements used for plate and 48 of elements used for six x -stiffeners.

Case 3. Two y -stiffeners are attached below the folded plate along transverse direction (Fig. 5c) with total mass increment of 9.78% (width of stiffening plate taken equal to 5cm and thickness remaining same as the original folded composite plate) with 192 of elements used for plate and 48 of elements used for two y -stiffeners.

Case 4. Six x -stiffeners and one y -stiffeners (which having the same geometry) are attached below the folded plate with total mass increment of 14.89% (Fig. 5d) with 192 of elements used for plate; 48 of elements used for six x -stiffeners and 24 of elements used for one y -stiffener.

The boundary conditions are

- Simply supported: at edges AB and CD: $u = v = w = \theta_x = 0$.
- Clamped: at edges AB and CD: $u = v = w = \theta_x = \theta_y = \theta_z = 0$.
- Cantilever plate: clamped all edges at $x = 0$ (except the edges of stiffeners).

3.3. Bending behaviors of stiffener orientations

The example deals with the effect of stiffener orientations on deflections of the plate subjected to a knife-edge loading $q = 10 \text{ kN/m}$, towards the negative direction of the z -axis (plotted in Fig. 5). The plates with constant thickness $t = 0.02\text{m}$ are considered in all cases.

Two boundary conditions: simply supported at edges AB, CD and clamped at edges AB, CD are taken for the analyses.

The deflections along the central line ($y = L$) of individual top plate for four cases are compared in Fig. 6 - Fig. 7 with the same scale for each.

+ For 5 plies $[45^\circ / -45^\circ / 45^\circ / -45^\circ / 45^\circ]$ with the same thickness $t_1 = t/5$.

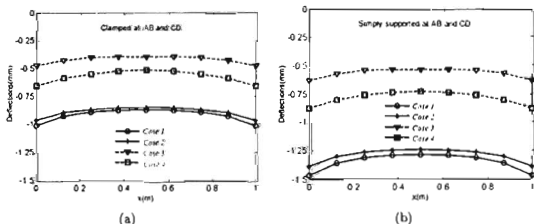


Fig. 6. Effects of stiffener orientation on deflections of the five folds folded composite plate, 5 plies $[45^\circ / -45^\circ / 45^\circ / -45^\circ / 45^\circ]$, thickness $t_1 = t/5$.

From Fig. 6 and Fig. 7, it is seen that the deflections of case 3 are least, although addition in mass is least in this case. The deflections of case 1 and case 2 are very closed to each others among all boundary conditions and layup sequences schemes. When case 2 is reinforced by one y -stiffener with a mass increment of about 4.78%, the deflection is significantly smaller than the one of before reinforcement. However, although total mass

increment of 14.78%, the deflections of case 2 are still higher than the deflections of case 3.

+ For 6 plies $[45^\circ / -45^\circ / 45^\circ / -45^\circ / 45^\circ / -45^\circ]$ with the same thickness of $t_i = t/6$.

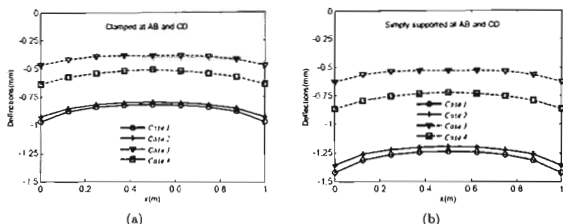


Fig. 7. Effects of stiffer orientation on deflections of the five folds folded composite plate, 5 plies $[45^\circ / -45^\circ / 45^\circ / -45^\circ / 45^\circ / -45^\circ]$, thickness $t_i = t/6$.

It is observed that case 3 is the best process of reinforcement for bending with the above loading scheme and case 2 is the worst process of reinforcement. For both of boundary conditions: clamped or simply supported at edges AB and CD, bending ability of the plate descended from case 3 to case 4, case 2 and case 1.

For symmetric and anti-symmetric in-axis configurations, bending behaviors of the plates are similar but they are giving less deflections.

3.3.1. Free vibration analysis

In this section, free vibration of the same unstiffened and stiffened five folds folded composite plate is carried out to investigate the effect of stiffener orientations. The boundary conditions are: simply supported at edges AB, CD and clamped at edges AB, CD; The lamination schemes are: symmetric: anti-symmetric in-axis configuration and off-axis configuration. Five first natural frequencies of the plates were computed and listed in Tab. 4 and Tab. 5 for the simply supported condition and clamped condition, respectively.

Five corresponding first mode shapes are available in Fig. 8 for the lay-up sequences $[45^\circ / -45^\circ / 45^\circ / -45^\circ / 45^\circ / -45^\circ]$ which giving comparisons of simply supported plate for different stiffeners orientations.

From Tab. 4 and Tab. 5, it is observed that, Case 3 gives the highest natural frequencies among the four cases, although addition in mass is least in the stiffened folded plates;

the natural frequencies of Case 2 (with total mass increment of 10%) are least. This phenomenon makes sense to us because the flexural rigidity of the plate should decrease as the effect of inertial momentum of x -stiffeners, for sure that we plotted the mode shapes of the plates in Fig. 8: natural frequencies of Case 4 do not make any significant change over the unstiffened folded plates, although total mass increment of 14.78%.

Table 4. Comparison of five first natural frequencies of five folds composite folded plate for various stiffeners conditions: simply supported at edged AB and CD, $t = 0.02$ m

Mode	[45°/-45°/45°/-45°/45°]				[0°/90°/0°/90°/0°]			
	Case 1	Case 2	Case 3	Case 4	Case 1	Case 2	Case 3	Case 4
1	5.52	5.24	8.46	7.11	10.12	9.56	13.87	10.63
2	25.47	24.63	38.62	32.08	37.63	36.13	46.15	29.15
3	38.41	37.52	45.41	40.02	47.32	45.04	63.24	50.86
4	56.53	54.17	85.34	71.15	90.78	86.73	110.71	65.98
5	78.76	77.57	96.74	84.06	101.36	96.02	132.76	107.34
Mode	[45°/-45°/45°/-45°/45°/-45°]				[0°/90°/0°/90°/0°/90°]			
	Case 1	Case 2	Case 3	Case 4	Case 1	Case 2	Case 3	Case 4
1	5.64	5.41	8.32	7.03	8.07	7.56	12.12	10.15
2	20.01	25.16	38.52	31.86	31.11	30.11	41.23	30.49
3	42.34	41.22	49.01	41.42	37.56	35.54	55.03	47.72
4	57.18	54.92	85.61	71.83	74.12	71.19	97.72	71.68
5	88.83	86.23	101.13	87.51	80.07	76.53	116.34	102.14

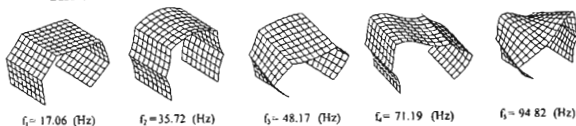
Table 5. Comparison of five first natural frequencies of five folds composite folded plate for various stiffeners conditions: clamped at edged AB and CD, $t = 0.02$ m

Mode	[45°/-45°/45°/-45°/45°]				[0°/90°/0°/90°/0°]			
	Case 1	Case 2	Case 1	Case 2	Case 1	Case 2	Case 1	Case 2
1	16.01	15.38	21.97	19.02	30.11	28.23	35.11	27.52
2	34.15	33.12	49.15	41.17	51.03	48.63	59.23	37.14
3	46.02	45.03	52.83	45.62	61.17	60.78	79.21	61.31
4	67.83	65.51	100.96	84.07	104.27	99.65	123.33	76.67
5	87.79	85.77	104.14	89.56	123.76	117.02	152.34	111.54
Mode	[45°/-15°/45°/-15°/45°/-15°]				[0°/90°/0°/90°/0°/90°]			
	Case 1	Case 2	Case 1	Case 2	Case 1	Case 2	Case 1	Case 2
1	17.06	16.32	22.01	18.69	23.61	22.21	30.03	27.01
2	35.72	31.18	49.28	42.32	41.34	40.02	51.18	40.26
3	48.17	46.71	53.79	47.15	50.79	48.03	69.17	60.72
4	71.19	68.02	101.42	85.36	84.01	81.73	108.37	82.16
5	91.82	91.73	108.88	93.62	97.75	92.97	132.83	117.51

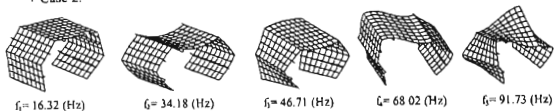
For Cases 1, 2 and 3, the natural frequencies of the plates having off-axis configurations are always lower than the frequencies of plates having in-axis configurations.

However, for Case 4, the second and fourth frequencies of off-axis plates are higher than the others because of the effect of y -stiffener initial momentum (for more clearly see the plotted mode shape in Fig. 8). We can also notice that the natural frequencies of the plates are significantly altered for y -stiffeners.

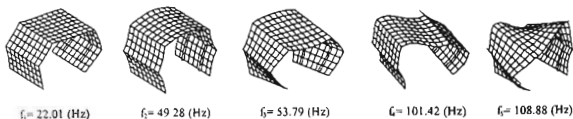
+ Case 1:



+ Case 2:



+ Case 3:



+ Case 4:

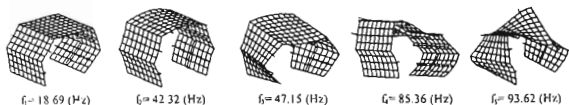


Fig. 8. First five mode shapes of simply supported; unstiffened and stiffened of the five folds folded composite plate, folding angle $\alpha = 120^\circ$, $[45^\circ / -45^\circ / 45^\circ / -45^\circ / 45^\circ / 45^\circ]$

For the same thickness and fiber orientation, when the number of ply increases the natural frequencies do not always increase (the second frequency of case 1; the second and third frequencies of Case 2 and Case 3 for simply supported condition are decrease).

It is observed that the effect of geometry of the folded plate on natural frequencies is significant.

Fig. 8 shows that the stiffeners do not make any change in getting mode shapes of presented plates (mode shapes make this study interesting, useful in dynamic analysis of the plates, but any generalized recommendation is very difficult without undergoing numerical experiments).

3.3.2. Transient response

In the analysis of transient response the same folded composite plates are subjected to an exploded knife-edge loading condition scheme of $q = 1$ kN/m, which having $t_1 = 1$ ms, $t_2 = 2$ ms, $t_3 = 50$ ms, illustrated in Fig. 9.

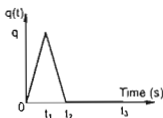
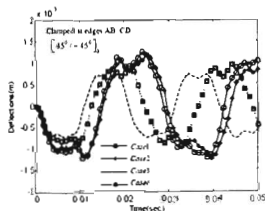


Fig. 9 Exploded loading condition scheme

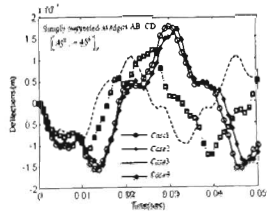
- Effect of stiffeners orientations

To observe the effects of stiffener orientations on transient displacement response, the plates having lamination schemes $[45^\circ/-45^\circ/45^\circ/-45^\circ/15^\circ/-15^\circ]$ and $[0^\circ/90^\circ/0^\circ/90^\circ/0^\circ/90^\circ]$ (denoted as $[45^\circ/-45^\circ]_3$ and $[0^\circ/90^\circ]_3$) are considered. The imposed boundary conditions simply supported and clamped at edges AB, CD. The results presented in the Fig. 10(a)-(d) have been compared for different cases.

Fig. 10(a) and Fig. 10(c) show the displacement response of point M (the center point of individual top plate) for clamped at edges AB, CD. Fig. 10(b) and Fig. 10(d) show the responses for simply supported at edges AB, CD.



(a)



(b)

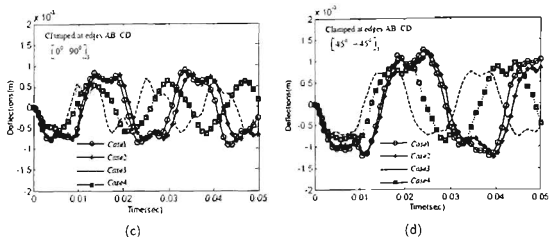
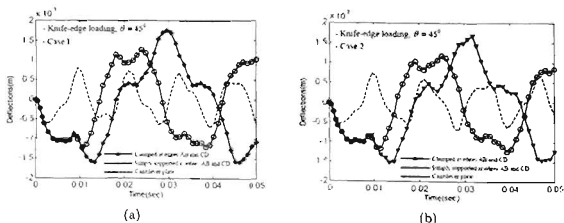


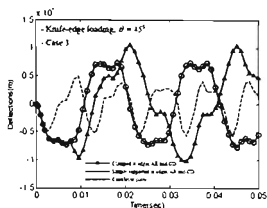
Fig. 10. Effects of stiffener orientations on transient displacement responses of the five folds composite folded plate, knife-edge loading condition, time step $\Delta t = 0.5(\text{ms})$

From Fig. 10, it can be observed that the displacement responses of Case 1 and Case 2 are closed to each other. The two y - stiffeners can be clearly improve the stiffness of the plate (Case 3) because of the deflection is decrease and the frequencies of the wave increase. The difference becomes more rapidly for simply supported plates. Furthermore, there is a significant increase of vibration frequencies when the plates having clamped at edges.

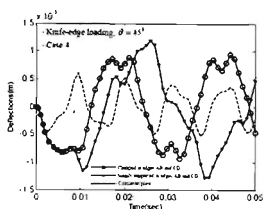
- Effect of boundary conditions

In this subsection, the effects of boundary condition on transient response of point M have been investigated for imposed boundary conditions: simply supported and clamped at edges AB CD; and clamped at $x = 0$ (cantilever plate). The plates having lamination schemes of $[45^\circ/-15^\circ/45^\circ/-15^\circ/15^\circ/-45^\circ]$ are taken to these analyses. The present results have been compared in Fig. 11(a)-(d) for four cases. From the Fig. 11, we found that the displacement amplitudes of cantilever plates are significantly lower than the ones of others boundary condition cases.





(c)



(d)

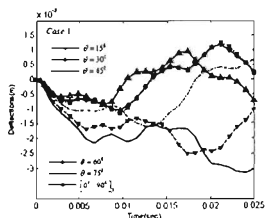
Fig. 11. Effects of boundary conditions on transient displacement responses of the five folds composite folded plate, knife-edge loading condition, time step $\Delta t = 0.5(\text{ms})$

- Effect of fiber orientations

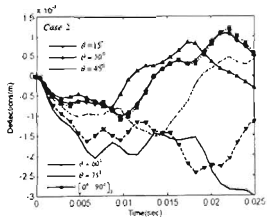
In this subsection, we investigated the displacement responses of the plate for various ply orientations of $\theta = 15^\circ, 30^\circ, 45^\circ, 60^\circ, 75^\circ$. The simply supported plate is subjected to a knife-edge loading scheme for duration time analysis of $T=0.025$ (sec). The lamination schemes $[\theta^\circ/-\theta^\circ/0^\circ/-\theta^\circ/\theta^\circ/-\theta^\circ]$ and $[0^\circ/90^\circ/0^\circ/90^\circ/0^\circ/90^\circ]$ (denoted as $[0^\circ/90^\circ]_3$) are taken.

The displacement responses of point M are calculated and plotted in Fig. 12 to show the influence of ply orientation for different cases.

From Fig. 12, it is seen that displacement responses of $[0^\circ/90^\circ]_3$ laminate plates and the plates having ply of $\theta = 15^\circ$ are closed. As the ply angle increases, the wave arrives at an earlier time and the frequencies of the wave increase. It can be concluded that a bigger ply orientation increases the stiffness in the axial direction, and speed of vibration extinction more quickly in that direction. The smallest displacement amplitude occurs for



(a)



(b)

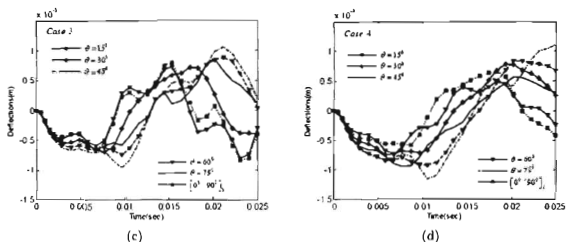


Fig 12. Effects of fiber orientations on transient displacement responses of the five folds composite folded plate, knife-edge loading condition, time step $\Delta t = 0.5(\text{ms})$, duration time $T = 0.025(\text{sec})$

the laminate with the ply angle of $\theta = 15^\circ$ because of the lowest bending stiffness in the lateral direction.

4. CONCLUSION

In this study, a finite element method using eight-noded isoparametric plate elements, based on the first order shear deformation theory was investigated for analysis of free vibration and transient response of the unstiffened and stiffened folded laminate composite plate by considering various parameters. The transverse shear deformation, rotary inertia of plate and stiffeners are considered in the present method to show the advantage of the model.

Generic validation studies dealing with isotropic stiffened, folded plates are undertaken to ensure the suitability of the present approach towards the unstiffened and stiffened folded laminate composite plate analysis.

Some set of new results are presented to see the effects of fiber orientations, loading conditions, boundary conditions, and fiber orientation on: bending deflections, natural frequencies, dynamic responses and mode shapes of unstiffened; stiffened folded laminate composite plates.

The applicability of the present approach covers a wide range of forced vibration problems, with varying material combinations, geometric features, and boundary conditions.

ACKNOWLEDGEMENT

This research is funded by Vietnam National Foundation for Science & Technology Development (NAFOSTED) under grant number: 107.02.2011.08.

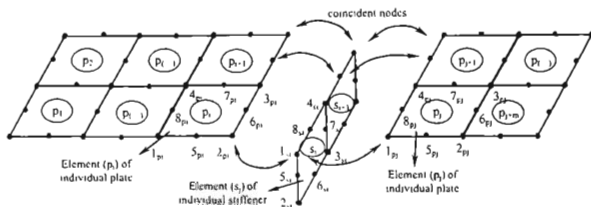
REFERENCES

- [1] Turkmen H. S., Mecitoglu Z., Dynamic response of a stiffened laminated composite plates subjected to blast load, *Journal of Sound and Vibration*, **221**, (1999), 371-389
- [2] Zhao X., Liew K M., Ng T. Y., Vibrations of rotating cross-ply laminated circular cylindrical shells with stringer and rings stiffeners, *Journal of Solids and Structures*, **39**, (2002), 529-545.
- [3] Sadek E. A., Tawfik S. A., A finite element model for the analysis of stiffened laminated plates, *Computers and Structures*, **75**, (2000), 369-383.
- [4] Kumar S. Y. V., Mukhopadhyay M., A new triangular stiffened plate element for laminate analysis, *Composites Science and Technology*, **60**, (2000), 935-943.
- [5] Olson M D., Hazell C. R., Vibration studies on some integral rib-stiffened plates, *J Sound Vibration*, **50**(I), (1977), 43-61.
- [6] Kollu M., Chandrashekhara K., Finite element analysis of stiffened laminated plates under transverse loading, *Composites Science and Technology*, **56**, (1996), 1355-1361.
- [7] Biswal K. C., Ghosh A. K., Finite element analysis for stiffened laminated plates using higher order shear deformation theory, *Computers and Structures*, **53**, (1994), 161-171.
- [8] Gangadhara Prusty, Linear static analysis of hat-stiffened laminated shells using finite elements, *Finite element in analysis and design*, **39**, (2003), 1125-1138.
- [9] Goldberg J. E., Leve H. L., Theory of prismatic folded structures, *Int. Assoc. Bridge and Structural Engng*, **17**, (1957), 58-86.
- [10] Bar-Yoseph P., Herscovitz I., Analysis of folded plate structures, *Thin-Walled Structures*, **7**, (1989), 139-158.
- [11] Cheung Y. K., Finite strip method of elastic slabs, *Proc*, ASCE **94**, (1968), 1365-1378.
- [12] Cheung Y. K., Folded-plate structures by finite strip method, *J. Struct. Div.*, ASCE **12**, (1969), 2963-2979.
- [13] Maleki S., Compound strip method for Box Girders and folded plates, *Comput Struct.*, **40**, (1991), 527-538.
- [14] Irie T., Yamada G., Kobayashi Y., Free vibration of a cantilever folded plate, *J Acoust. Soc. Am.*, **76**(5), (1984), 1743-1748.
- [15] Perry B., Bar-Yoseph P., Rosenhouse G., Rectangular hybrid shell element for analysing folded plate structures, *Computers and Structures*, **44**, (1992), 177-183.
- [16] Kutlu Darilmaz, Nahit Kumbasar, An 8-node assumed stress hybrid element for analysis of shells, *Computers and Structures*, **84**, (2006), 1990-2000.
- [17] Haldar S., Sheikh A. H., Free vibration analysis of isotropic and composite folded plates using a shear flexible element, *Finite Elem. Anal. Des.*, **42**, (2005), 208-226.
- [18] Suresh R., Malhotra S. K., Vibration and damping analysis of thin-walled box beams, *J. Sound Vib.*, **215**, (1998), 201-210.
- [19] Sreyashi Pal., Guha Niyogi, Application of folded formulation in analyzing stiffened laminated composite and sandwich folded plate vibration, *Journal of Reinforced Plastics and composites*, **27**, (2008), 692-710.
- [20] Bui van Binh, Tran Ich thinh, Tran Minh Tu, Analysis of bending folded laminated composite plate by finite element method, *International conference on Science and Technology*, Science and Technics Publishing House, Session **6**, (2011), 711-723.
- [21] Tran Ich Thinh, Bui Van Binh, Tran Minh Tu, Vibration of folded laminate composite plate, *International conference on Science and Technology*, Science and Technics Publishing House, Session **6**, (2011), 659-670.
- [22] Tran Ich Thinh, Bui Van Binh, Tran Minh Tu, Static and free vibration of laminated composite folded plate using finite element method, *Journal of Science and Technology*, **49**(2), (2011)

- [23] Tran Ich Thinh, Bui Van Binh, Tran Minh Tu, Bending and Vibration analyses of multi-folding laminate composite plate using finite element method, *Vietnam Journal of Mechanics*, **34**(3), (2012).
- [24] Singiresu. S. Rao, *The Finite Element Method in Engineering*, Elsevier, (2004).
- [25] Tran Ich Thinh, Ngo Nhu Khoa, *Finite element method*, Science and Technics Publishing House, (2007).
- [26] Tran Ich Thinh, *Composite Materials*, Vietnam Education Publishing House, (1994).
- [27] Bathe, K-J, *Finite element procedures*, Prentice-Hall, Inc, (1996).

Received April 11, 2012

APPENDIX



The degrees of freedoms between the plate and stiffener at the intersection are coincident.

For example: node (2_{p_i}) of element p_i ; node (1_{s_i}) of element s_i and node (1_{p_j}) of element p_j are coincident. It is similar for nodes $(6_{p_i}$; 8_{s_i} and $8_{p_j})$ and for nodes $(3_{p_i}$; 4_{s_i} and $4_{p_j})$,...